Journal of Hydrology X 15 (2022) 100125

Contents lists available at ScienceDirect

Journal of Hydrology X

journal homepage: www.sciencedirect.com/journal/journal-of-hydrology-x

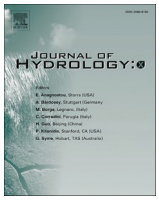

Research papers

Complex wave propagation from open water bodies into aquifers: A fast analytical approach

Wout Hanckmann [a], Thomas Sweijen [a,b], Alraune Zech [a,*]

[a] Department of Earth Sciences, Utrecht University, Princetonlaan 8a, Utrecht 3584CB, The Netherlands
[b] Crux Engineering BV, Pedro de Medinalaan 3c, Amsterdam 1086XK, The Netherlands

ARTICLE INFO

Keywords:
Hydraulic diffusivity
Coastal aquifers
Wave propagation
Analytical solution
Parameter estimation

ABSTRACT

Aquifers are of particular interest in the vicinity of rivers, lakes and coastal areas due to their extensive usage. Hydraulic properties such as transmissivity and storativity can be deduced from periodical water level fluctuations in both open water bodies and groundwater. Here, we model the effect of complex wave propagation into adjacent isotropic and homogeneous aquifers. Besides confined aquifers, we also study wave propagation in leaky aquifers and situations with flow barriers near open water bodies as encountered in harbours where sheet piling are in place. We present a fast analytical solution for the hydraulic head distribution which allows for determining the hydraulic diffusivity (S_s/K) of the aquifer, with low investigational efforts. We make use of the Fast Fourier Transform to decompose complex wave boundary conditions and derive solutions through superposition. Analytical solutions are verified by comparing to numerical MODFLOW models for three application examples: a tidal wave measured in the harbour of Rotterdam, a synthetic square wave and river fluctuations in the river Rhine near Lobith. We setup a parameter estimation routine to identify hydraulic diffusivity, which can be easily adapted to real observation data from piezometers. Inverse estimates show relative differences of less than 2% to numerical input data. A sensitivity study further shows how to achieve reliable estimates depending on the piezometer location or other influencing factors such as resistance values of the confining layer (for leaky aquifers) and flow barriers.

1. Introduction

Coastal areas are becoming increasingly important for social and economic activities as they furnish a wide range of human activities such as tourism, recreation, transport, and fisheries (EPA, 2008). Thus, they are subjected to urbanization and a variety of subsurface engineering activities whilst they have a complex hydrogeology. Example projects include topics as flood risk mitigation, contaminant remediation, measure against seawater intrusion, drinking water management and underground construction developments. The hydrogeology of coastal areas is often found to be dominated by tidal waves propagating into aquifers, yielding a complex dynamic groundwater system. Thus, engineering in coastal areas requires a good knowledge of the hydrogeological conditions and parameters.

For aquifer characterization, pumping tests are a well-established tool that are available at small-scale (i.e. slug tests) and intermediate-scale (i.e. pumping tests by several wells and piezometers) (Kruseman and de Ridder, 2000; Houben, 2015). They yield information on aquifer characteristics such as storativity S and transmissivity that can be used to find hydraulic conductivity K when the aquifer thickness d is known. However, pumping tests require a substantial effort while identified parameters represent a limited aquifer volume. In that respect analysing the tidal wave signal in coastal aquifers can be a valuable method to identify hydraulic parameters valid for large scale aquifer volumes.

Ferris (1951) proposed wave signals to estimate hydraulic parameters in coastal and riverine aquifers through reverse analysis using an analytical solution. The latter describes a simple wave propagating in a semi-infinite homogeneous confined aquifer. This approach also holds for unconfined aquifers when the saturated thickness is much larger than the wave's amplitude (Bear, 1972; Li and Jiao, 2002). This solution makes use of the hydraulic diffusivity $\frac{S_s}{K}$, being the ratio of specific storage S_s and hydraulic conductivity K. Even though diffusivity does not allow to identify both, S_s and K, it is a useful parameter to estimate being used in time-dependent pumping equations (Theis, 1935). Especially, combining an analysis of the wave propagation with a pumping test can provide additional information on aquifer properties to increase

* Corresponding author.
E-mail address: a.zech@uu.nl (A. Zech).

https://doi.org/10.1016/j.hydroa.2022.100125
Received 7 December 2021; Received in revised form 2 March 2022; Accepted 3 April 2022
Available online 11 April 2022

parameter estimation reliability. Many analytical solutions have been developed for more complex hydrogeological situation of coastal aquifers. For example, Nielsen (1990) included the effect of a sloping beach for a single aquifer system; Sun (1997) derived a 2-dimensional solution to investigate tidal effects in estuaries; Jiao and Tang (1999) introduced the effect of leakage assuming a constant sea-level in the aquifer topping the confining layer; Li and Jiao (2002) extended this concept of leakage to a vertical two-aquifer system by including wave interference between the layers; Sun et al. (2008) added a second tidal boundary condition to the solution of Jiao and Tang (1999) making their solution applicable for islands and peninsulas; and finally Guo et al. (2007);Guo et al. (2010) analysed a two-zone system with a confined aquifer split up horizontally in two areas with different $\frac{S_s}{K}$ ratios. These solutions are most likely capable of performing inverse analysis to determine $\frac{S_s}{K}$ from field data for particular input wave situations: a simple sinusoidal wave or superpositions of diurnial and semi-diurnial tidal components.

However, waves in coastal and riverine areas often cannot be described by a superposition of known diurnial and semi-diurnial components as they are highly irregular due to complex basin geometry in e.g., estuaries or harbours (Nidzieko, 2010). Additionally, many open water bodies such as rivers, artificial lakes and locks show fluctuations that are not driven by tidal forces. This limits the usage of the listed analytical solutions to very specific problem definitions.

To overcome these limitations, we derive analytical solutions for complex wave boundary conditions making use of superposition given the linearity of governing equations. For this purpose, we use Fast Fourier Transformation (FFT) to decompose the input wave. The analytical solution is versatile and can be used for any boundary conditions providing they are continuous. Novel solutions will allow determining diffusivity $\frac{S_s}{K}$ for confined homogeneous aquifer systems without and with leakage. They can thus be used for many practical applications alongside or prior to extensive field testing, e.g. with pumping tests and numerical modelling.

The analytical solutions are tested against numerical simulations of the same conceptual aquifer setup with complex wave boundary conditions to show the reliability of the solution's performance. We further make use of numerical data as artificial measurements to establish an inverse parameter estimation procedure. Solutions are tested in detail on their sensitivity on the piezometer location and influencing factors such as resistance values of the confining layer and flow barrieres.

The course of the paper is the following: in Section 2, we specify a conceptual model, introduce simple wave solutions that are available in literature from which we derive the complex wave solutions, setup the numerical model and parameter estimation procedure. Results are discussed in Section 3 for both, the confined aquifer solution and the situation of leakage. We close with a summary and conclusion. Additional information is available in the *Supporting Information*.

2. Methods and Data

2.1. Conceptual Model

We consider a horizontal confined aquifer near an open water body such as a river, harbour or lake. The confined aquifer is separated from the overlaying unconfined aquifer through a confining or leaky aquitard such as a clay or peat layer, as displayed in Fig. 1. We study two settings in details, which are often encountered in practice: (i) fully confined aquifer (without leakage); and (ii) a leaky confining layer, resulting in a hydraulic contact between the confined and the overlaying unconfined aquifer. We further test the applicability of our approach on the situation of a low-permeable barrier separating the aquifer from the open water such as a quay wall or sheet-piling found in harbours or canals.

Major assumptions are: (i) aquifers are isotropic and homogeneous in their hydraulic properties, including hydraulic conductivity K and specific storage S_s; (ii) aquifers and open water bodies are separated by a sharp vertical interface with small lateral extent compared to the distance of wave propagation; (iii) flow in the confined aquifer is horizontal and free of density driven flow.

In case of a leaky aquifer, we assume vertical flow to be linearly proportional to the head difference between the confined and unconfined aquifer. The storage of the leaky confining layer is negligible, which is a commonly used assumption in layered coastal aquitards (Hemker, 1999). The water table in the unconfined aquifer is constant and equals the mean sea-level. This setting is based on the assumption that the wave is either damped quickly given the large storage capacity or not propagating into the unconfined layer at all such as in controlled situations like polders where pumps guarantee a constant water level (Jiao and Tang, 1999).

2.2. Mathematical Model

2.2.1. Simple Wave Boundary Solution

The hydraulic head in a confined aquifer is given by a solution of the following partial differential equation (Ingersoll et al., 1948):

$$S_s \frac{\partial h(x,t)}{\partial t} = K \frac{\partial^2 h(x,t)}{\partial x^2}, \tag{1}$$

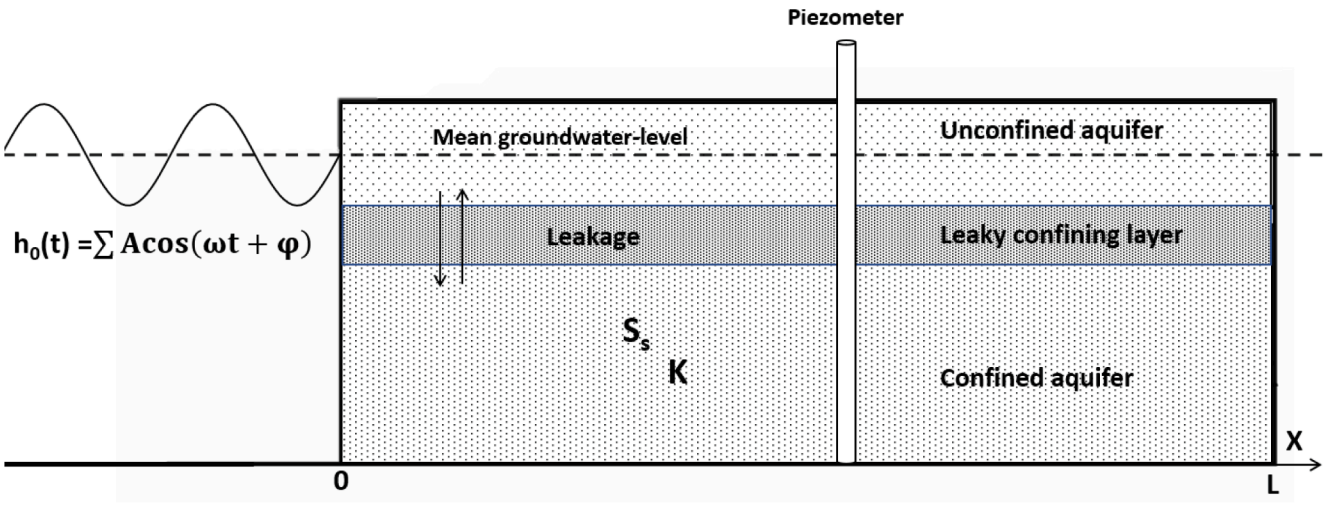

Fig. 1. Conceptual aquifer model in the domain $x \in [0, L]$. Fluctuations in water level, $h_0(t)$, in an open water body at $x = 0$. The confined aquifer has a hydraulic conductivity K and specific storage S_s. This Figure also shows the setup of the piezometer and potential leakage from an unconfined overlaying aquifer.

where $h(x,t)$ [m] is the spatio-temporal hydraulic head profile in time t [d] and distance x [m] from the open water body, S_s [1/m] is the specific storage, and K [m/d] is the horizontal hydraulic conductivity.

For the case of a confined aquifer with leakage from an unconfined aquifer through a semipermeable layer, the equation extends to (Jiao and Tang, 1999)

$$S\frac{\partial h(x,t)}{\partial t} = T\frac{\partial^2 h(x,t)}{\partial x^2} + \frac{1}{c_L}[h_s - h(x,t)], \tag{2}$$

with $S = S_s{\cdot}d$ [m] being the storativity, $T = K{\cdot}d$ [m^2/d] the aquifer's transmissivity where d [m] is the confined aquifer thickness; c_L [d] the resistance of the confining layer, which is the thickness of the confining layer divided by its hydraulic conductivity; h_s [m] is the wave's equilibrium constant, which corresponds to the outer boundary condition of the semi-infinite aquifer, i.e. $h(x=\infty,t) = h_s$. We assume $h_s = 0$ for the sake of simplicity.

The impact of the open water body is described by a time-dependent boundary condition (BC) at $x = 0$ via:

$$h_0(t) = A\cos(\omega t + \varphi) + h_s, \tag{3}$$

where A [m] is the tidal wave amplitude, ω [rad/d] is the angular frequency and φ [rad] is the phase shift. The general solution of the partial differential Eqs. (1) and (2) for the simple wave BC (3) reads (Ingersoll et al., 1948; Jiao and Tang, 1999):

$$h(x,t) = A\exp(-Bx)\cos(\omega t + \varphi - Cx) + h_s, \tag{4}$$

with variables specific to each solution (confined and leaky): $B = C = \sqrt{\frac{\omega}{2}\frac{S_s}{K}}$ for the confined aquifer without leakage (Eq. 1) and $B = \sqrt{\frac{\omega}{2}\frac{S}{T}}\widetilde{p}$ and $C = \sqrt{\frac{\omega}{2}\frac{S}{T}}\frac{1}{\widetilde{p}}$ for the leaky aquifer situation (Eq. 2) with $\widetilde{p} = \sqrt{\sqrt{\frac{1}{(c_L S\omega)^2}+1} + \frac{1}{c_L S\omega}}$. Note that for infinite resistance, $\widetilde{p}$ becomes one and thus reproducing the confined aquifer solution.

2.2.2. Complex Wave Boundary Solution

An arbitrary wave boundary function $h_0(t)$ can be decomposed into simple waves by Fourier decomposition as an infinite sum of singular waves, each with amplitude A_k, frequency ω_k and phase shift φ_k:

$$h_0(t) = \sum_{k=0}^{\infty} A_k\cos(\omega_k t + \varphi_k) + h_s \tag{5}$$

Given the linearity of the governing Eqs. (1) and (2) for the head distribution in confined and leaky aquifers, solutions for a complex wave BC (5) can be created through linear superposition of the simple wave solution (4) to:

$$h(x,t) = \sum_{k=1}^{n} A_k\exp(-B_k x)\cos(\omega_k t - \varphi_k - C_k x) + h_s \tag{6}$$

with $B_k = C_k = \sqrt{\frac{\omega_k}{2}\frac{S_s}{K}}$ for the confined aquifer without leakage and for the leaky aquifer situation $B_k = \sqrt{\frac{\omega_k}{2}\frac{S}{T}}\widetilde{p}_k$ and $C_k = \sqrt{\frac{\omega_k}{2}\frac{S}{T}}\frac{1}{\widetilde{p}_k}$ with $\widetilde{p}_k = \sqrt{\sqrt{\frac{1}{(c_L S\omega_k)^2}+1} + \frac{1}{c_L S\omega_k}}$.

The complex wave boundary solutions (6) (for confined and leaky aquifers) are implemented in an accompanying open-source `Python` package making use of FFT. The critical step for identifying the solution of the head $h(x,t)$ is the decomposition of the input wave $h_0(t)$ (Eq. 5) via FFT and identifying amplitudes, frequencies and phase shifts of each wave component. Technical details are provided in the *Supporting Information*.

2.3. Numerical Model

The propagation of complex waves into aquifers can also be solved numerically. For proof of concept and for generating artificial reference data, we setup flow models in MODFLOW 2005 (Harbaugh, 2005) through the python package `FloPy` (Bakker et al., 2016).

We prepared several model setups: a regular confined aquifer and a leaky aquifer setting following the conceptual model outlined in Section 2.1. The choice of parameters is given in Table 1. We further setup a numerical model for a low-permeable barrier between the confined aquifer (without leakage) and the open water body. The resistance to groundwater exchange, is approximately the ratio of an effective thickness d_B and an effective hydraulic conductivity K_B of the barrier. Its specific storage equals that of the confined aquifer. The numerical model results of this scenario are used to identify limits of the applicability of the confined aquifer solution (Eq. 6) for this particular flow situation.

We run the numerical model for three types of complex wave boundary conditions, which are visualized in Fig. 2: (i) a tidal wave as typically observed in harbours, (ii) a synthetic square wave, and (iii) an observed fluctuating river level. The times series are normalized to an average of $h_s = 0$ over the observation interval.

The aquifer system is discretized through a one-dimensional grid of 15,000 cells with exponentially increasing grid spacing. The grid spacing is adapted to the strong head fluctuation close to the open water body, which decreases with distance. It thus allows for a better resolution of the head while limiting the amount of memory needed for the constant head boundary at infinite distance. Observations of the head in the aquifer are taken at multiple distances x mimicking observation wells. Simulation time T_{sim} varies between 5 and 480 days, depending on the length of the time series of the BCs (Fig. 2). Observations times are identical to those given by the time series.

2.4. Parameter Estimation

The analytical solution (6) can be used to estimate aquifer specific parameters, such as the hydraulic diffusivity $\frac{S_s}{K}$, under the condition that at least two time series of measurements are available, namely that of piezometric heads in the aquifer and water level observations of the open water body. We consider the numerical model results as artificial observations and test the efficiency of the analytical solution for inverse parameter estimation through fitting. In case of leakage, a second unknown parameter is the product of resistance and storativity $c_L{\cdot}S = c_L S_s d$.

We apply an inverse estimation procedure which focuses on dominant wave components to reduce wave noise effects. The workflow has the following steps:

1. Decompose the particular complex wave boundary condition $h_0(t)$ (which is assumed to be known) with FFT to identify amplitudes A_k^0, frequencies ω_k^0 and phase shifts φ_k^0.

Table 1
Hydrogeological parameters characterizing numerical aquifer models: first parameters for all models, then parameters for leaky aquifer (subscript L) and for the flow barrier at $x = 0$ (subscript B).

Parameter	Value
Aquifer length L	10 km
Hydraulic conductivity confined aquifer K	25 m/d
Specific storage confined aquifer S_s	$5{\cdot}10^{-5}$ m^{-1}
Thickness confined aquifer d	10 m
Resistance confining layer c_L	$[1, 10^5]$ d
Thickness confining layer d_L	1 m
Hydraulic conductivity unconfined layer K_u	25 m/d
Specific yield unconfined layer S_y	0.25 [-]
Resistance barrier c_B	$[10^{-3}, 10]$ d
Thickness barrier d_B	0.1 m

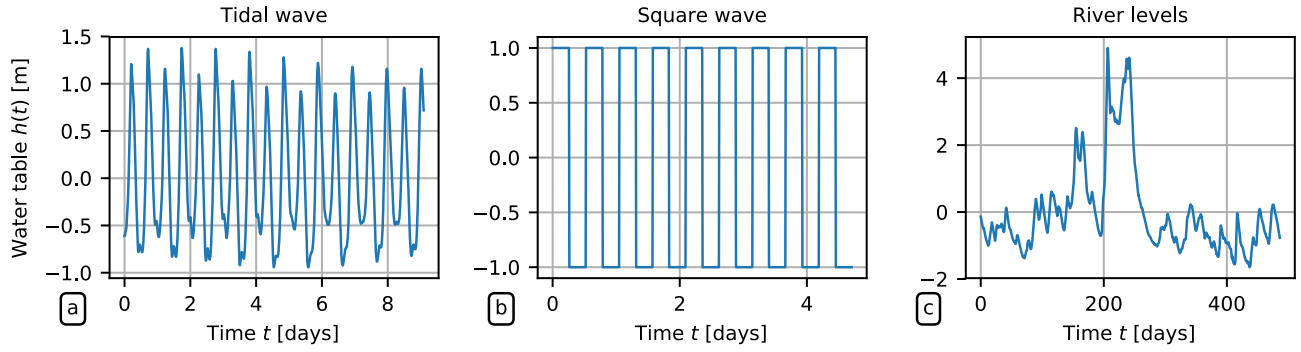

Fig. 2. Boundary conditions used: (a) tidal wave measured in Europahaven Rotterdam, the Netherlands, (b) synthetic square wave, (c) river levels of the Rhine at Lobith, the Netherlands.

2. Identify the dominant wave component of $h_0(t)$ being the one with the largest amplitude $A^0_{\max}$.Select all wave components ($A^0_{\text{thres}}, \varphi^0_{thres}$, and ω^0_{thres}), which are at least 20% relative to the dominant amplitude.The threshold value of 20% is arbitrary but proofed useful since the quality of the fit goes down when all FFT components are used.
3. Decompose the head time series $h_x(t)$ at a piezometer position x via FFT. In our case of full data availability from the numerical model, we select time series $h_x(t)$ at reasonable distances x.
4. Identify the FFT decomposition components ($A^x_{\text{thres}}, \varphi^x_{thres}$, and ω^x_{thres}) of the decomposed head time series $h_x(t)$, which correspond to the threshold wave components of the input wave FFT decomposition. This is possible since ω_{max} does not change with x and t during propagation through the aquifer linking the FFT decomposition of $h_0(t)$ and $h_x(t)$.
5. Reconstruct the wave at x via $h^{\text{thres}}_x(t) = \sum_i A^x_{\text{thres(i)}} \cos\left(\omega^x_{\text{thres(i)}} t + \varphi^x_{\text{thres(i)}}\right)$.
6. Setup the analytical wave solution $h^{\text{thres}}\left(t, \frac{S_s}{K}\right)$ for the selected wave components according to Eq.6.
7. Run a minimization routine to identify the optimal $\frac{S_s}{K}$ by fitting the difference between the observed wave (of dominant components) $h^{\text{thres}}_x(t)$ to the function $h^{\text{thres}}\left(t, \frac{S_s}{K}\right)$.

The workflow is implemented in the accompanying `Python` package. For optimization we use simple least square fitting through the routine `curve_fit`. The procedure is similarly applicable to real head observations at x and wave observations in an open water body.

We evaluate estimated parameters, particularly diffusivity $\frac{S_s}{K}$ by comparison to the input value of the numerical model making use of the relative difference $\varepsilon_{\text{rel}}(y) = \frac{|y^{\text{ana}} - y^{\text{num}}|}{y^{\text{num}}}$, where y stands for a particular parameter.

The quality of the parameter estimation is a function of the FFT decomposition and depends on the location x of the observation well. The depth of the wave propagation into the aquifer depends on the wave frequency. Furthermore, the wave signal is damped during propagation through the aquifer, shown in decreasing wave amplitudes. This effect is amplified by leakage. We quantify the impact of distance and damping on the estimation quality through a damping coefficient ζ^x_{max} which relates the largest amplitudes of the input wave and the observed one:

$$\zeta^x_{max} = 1 - \frac{A^x_{\max}}{A^0_{\max}} \in [0, 1] \tag{7}$$

3. Results and Discussion

3.1. Confined Aquifer Solution

3.1.1. Analytical Solution Performance

The first step of finding a solution for a wave progagation into an aquifer (Eq. 6) is the decomposition of the complex wave itself (Eq. 5). The implementation of the FFT decomposition of $h_0(t)$ is tested and reported in the *Supporting Information*, where we show that the decomposed BC reproduces the input time series for all three selected waves very well.

After decomposition of $h_0(t)$, the head distribution in a confined aquifer is computed for the three boundary waves, using the analytical solution. Results are subsequently compared to their numerical counterparts, i.e. the results from MODFLOW simulations. Fig. 3 shows the head distributions in space $h(x)$ at selected times, normalized to the simulation time such that: $T = t/T_{\max} \in [0, 1], T_{\max}$ corresponds to the end observation time of the wave input BC.

Both, the numerical and analytical solutions agree very well for all three wave BCs and times. The very good performance of the analytical solution makes it a simple method for computing wave propagation of complex waves in aquifers. It further provides an application tool for parameter estimation based on piezometer time series.

3.1.2. Inverse Parameter Estimation

We test the analytical solution (6) for a confined aquifer and for all three wave BCs (Fig. 2) through fitting it to the numerical data using the procedure outline in Section 2.4. We selected the piezometer to be located at $x = 400$m from the open water body.

Fig. 4 shows the results of the fitting of the analytical solution to its numerical counterpart, which are of good quality. The estimates of the hydraulic diffusivity $\frac{S_s}{K}$ showed a relative difference ε_{rel} of less than 2% for all input waves.

3.1.3. Impact of Observation Location

The quality of inverse parameter estimation results depends on the location of the piezometer to the boundary. Fig. 5 shows the effect of the location of the piezometer on the diffusivity estimate through the relative differences between the fitted and model input diffusivity as function of the piezometer location x and the damping coefficient (Eq.7) for all three wave BC. Note that the damping coefficient can better be interpreted as a re-scaling of the distance x with regard to the impact of the dominant wave amplitude.

In case of the tidal boundary condition, the relative error ε is low, except for piezometers in the vicinity of the open water body ($x = 0$) and for locations far from the open water body. Thus, an optimum range exists at intermediate distances. The same holds for the river level BC,

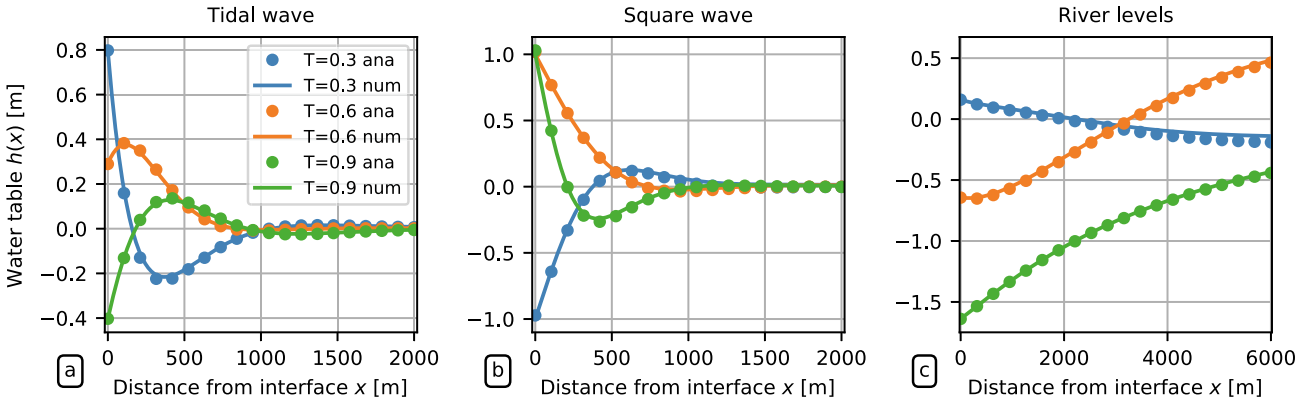

Fig. 3. Hydraulic head distributions $h(x)$ at three relative times $T = t/T_{\max}$ for the numerical model (lines) and analytical solutions (dots) under confined flow conditions for the three wave BCs: (a) tidal wave, (b) square wave, (c) river levels.

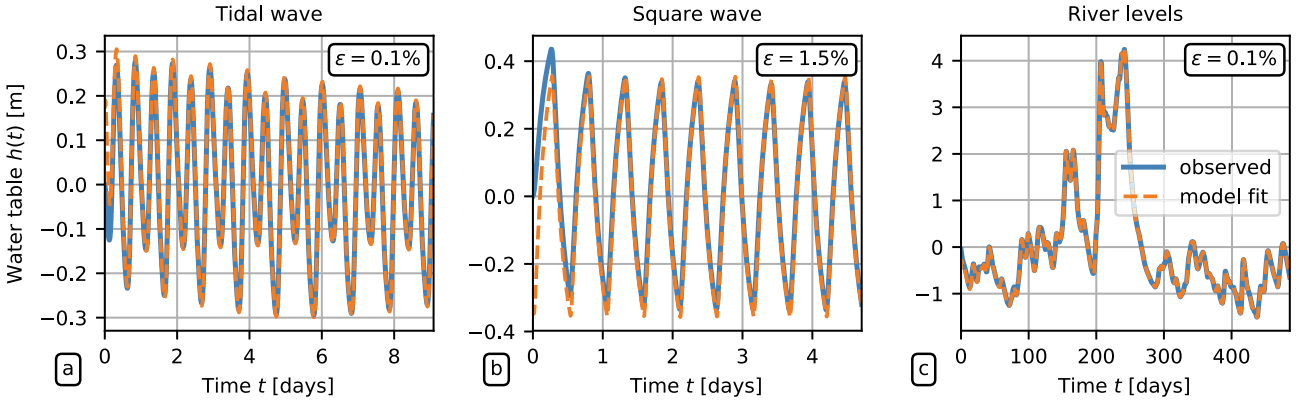

Fig. 4. Fit of the analytical solution (orange) to the numerical solution (blue) for the piezometric head data observed at $x = 400$ m under confined flow conditions for the three wave BCs: (a) tidal wave, (b) square wave, (c) river levels. ε denotes relative difference between input and estimated hydraulic diffusivity $\frac{S_s}{K}$.

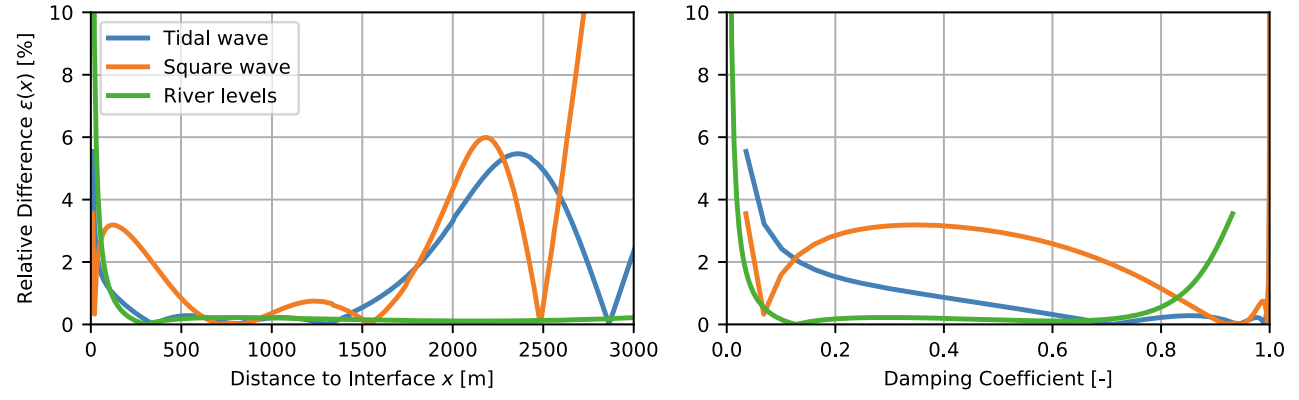

Fig. 5. The relative difference of fitted to model input diffusivity $\frac{S_s}{K}$ as function of the distance x of the observation well to the open water body and as function of the damping coefficient ζ.

while here the distance x for increasing relative differences is much higher. This is due to the different character of the time series being of larger wave length penetrating deeper into the aquifer.

The behaviour is confirmed by the damping coefficient relation. Close to $x = 0$, the input wave is hardly damped and shows high amplitudes. Thus, the aquifer had little effect on the groundwater fluctuations at small distances from the boundary and the analytical solution is highly sensitive towards deviations in the estimate of $\frac{S_s}{K}$, resulting in high

relative differences. At the other hand, at large distances from the boundary the damping coefficient increases causing the propagating wave to be hardly detectable in the field, inhibiting an accurate estimate. Estimates are typically best for relatively short distances x, when damping of the signal has not progressed to much but has progressed far enough for the aquifer to have an effect.

The relative difference of $\frac{S_s}{K}$ in case of the square wave is low for all damping coefficients. We relate that to the regular structure of the square wave and the sufficient input BC time series length. The wave quickly propagates through the aquifer and the dominant amplitude can be identified properly at all distances. Thus, the agreement of analytical with numerical solution is high and so is the quality of the diffusivity estimate.

3.2. Leakage and Flow Barriers

In many field situations the boundary wave propagation in an confined aquifer is impacted by specific conditions such as leakage through the confining layer or vertical flow barriers along the open water bodies. Both are characterised by a specific resistance c which is linked to the local hydraulic conductivity K of the leaking confining layer (subscript L) or flow barrier (subscript B), respectively: $K_L = d_L/c_L$ and $K_B = d_B/c_B$ where d is the thickness of the specific layer. For further analysis of the impact of leakage and barriers we focus on the tidal wave input BC.

3.2.1. Robustness of Confined Aquifer Solution

We first tested robustness of the analytical solution (Eq. 6) for confined aquifers (not considering the impact of leakage and barriers explicitly) by comparing it to numerical model results taking leakage and flow barriers into account for a wide range of resistance values using the tidal wave BC. We estimated diffusivity through the inverse estimation procedure (Section 2.4) and plotted the relative difference to input diffusivity in Fig. 6. It is displayed as function of the ratio of conductivity of the leaking semi-impermeable layer, or barrier respectively, and the confined aquifer conductivity.

Results in Fig. 6(a) show that the flow behaviour for leaky aquifers starts to deviate from confined aquifer behaviour when the conductivity of the confining layer K_L is less than four orders of magnitude smaller than the confined aquifer conductivity K. At this threshold, the estimate of diffusivity starts deviating from the input value by more than 10% rendering the estimate unreliable. The deviation increases with increasing distance x of the observation location given the damping effect of leakage on the wave traveling through the aquifer.

For the situation of a flow barrier (Fig. 6b), the estimates of diffusivity are reliable for a range of two order of magnitude differences between the flow barrier K_B and the aquifer conductivity K. When the resistance of the barrier is much higher, i.e. the conductivity goes down, then the input wave is highly damped and the observed signal cannot be matched to the confined aquifer solution, as expected.

The comparison in Fig. 6 shows the range of resistance values for which leakage and flow barriers do not significantly impact how the input wave BC travels through the confined aquifer. Given the chosen numerical model values of confined aquifer conductivity K and layer thickness d (Table 1), this refers to resistances of $c_L = 400\,\mathrm{d}$ and $c_B = 0.4\,\mathrm{d}$. Results show that both aspects have very distinct and partially counteracting influence on the wave propagation. Thus, we expect the wave signal for an aquifer exposed to leakage and a flow barrier at the same time as a superposition of both influences.

For strongly leaking confined layers, the use of the analytical solution including the effect of leakage can be used to identify reliable estimates of diffusivity (see following section). In case of a flow barrier along the open water body, we do not consider the use of an adapted solution. Instead, it is more efficient to observe the actual signal behind the flow barrier, e.g. in a piezometer at a few meter distance to the barrier, and use that as input BC signal for the confined aquifer solution.

3.2.2. Inverse Parameter Estimation for Leaking Aquifers

The analytical solution for leaky aquifers (Eq. 6) also shows good agreement to the numerical results of the MODFLOW model for the same setting. Results analog to Fig. 3 are displayed in the *Supporting Information*. A significant feature of leakage is the damping of the wave propagation into the aquifer, due to groundwater exchange through leakage. Thus, locations for inverse parameter estimation need to be adapted and closer to the open water body.

As shown in the previous section, the head distribution is significantly impacted by leakage for confining layer resistances c_L smaller than 400 days. We ran the fitting procedure to numerical simulation results estimating diffusivity $\frac{S_s}{K}$ and the resistance factor $c{\cdot}S$ simultaneously for various distances of the piezometer from the open water body given the strong impact of leakage on damping the wave signal. Results are displayed in Fig. 7.

The pattern of inverse estimation quality of diffusivity and resistance factor $c{\cdot}S$ in Fig. 7 strongly depends on the leakage factor and observation distance. Generally, the reliablity of the inverse estimate of diffusivity decreases with decreasing resistance value c due to the stronger damping effect of leakage while the estimate of the leakage factor $c{\cdot}S$ becomes less reliable for increasing resistances c. Observation

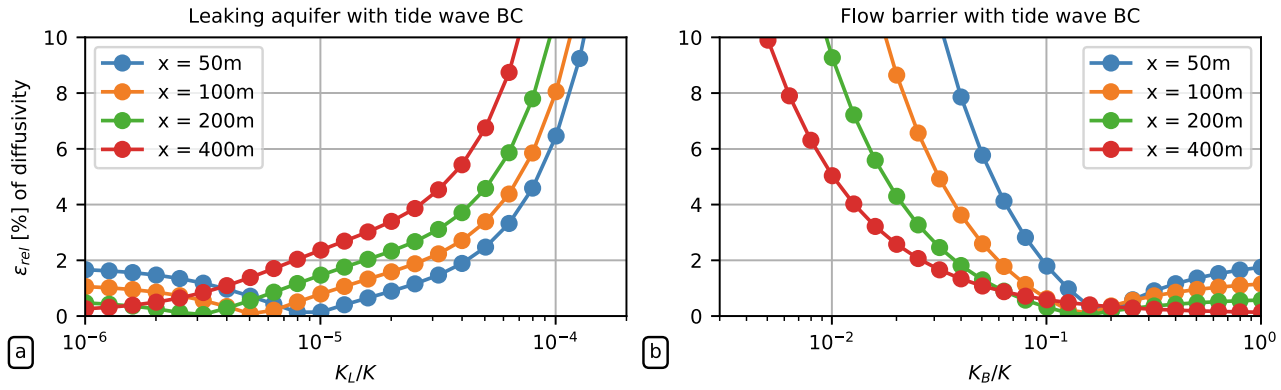

Fig. 6. The relative difference of the fitted diffusivity $\frac{S_s}{K}$ using the confined aquifer solution for MODFLOW model results including leakage (left) and a flow barrier (right) over a range of local conductivity values. Results refer to the tidal wave BC, numerical input values are listed in Table 1 and are taken at various distances x from the open water body.

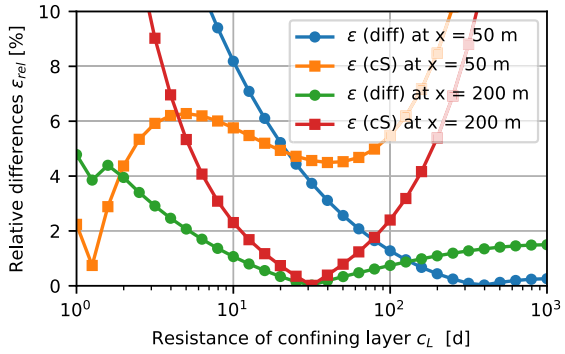

Fig. 7. Relative difference of the fitted diffusivity $\frac{S_s}{K}$ and leakage factor $c_L \cdot S$ for inverse estimation at two distances $x = 50\,\text{m}$ and $x = 200\,\text{m}$ using the analytical solution considering leakage for the tidal wave BC.

locations at larger distances, e.g. $x = 200\,\text{m}$ are better for estimating diffusivity, while the leakage factor is only well estimated for a small range of values. Closer to the open water body, e.g. at $x = 50\,\text{m}$, the estimate of resistance is particularly better for very small resistances which is linked to the rapid damping of the wave signal for strong leakage.

4. Summary and Conclusions

We investigated analytical solutions for the propagation of complex waves in confined and leaky homogeneous aquifers, close to open water bodies, such as rivers, lakes, and coastal areas. We derived explicit mathematical expressions for the hydraulic head in aquifers as function of time, location from the open water body and the input wave signal. Solutions are implemented in an accompanying open source `Python` package making use of Fast Fourier Transformation. The solutions are tested for three application examples: a tidal wave, a synthetic square wave and river fluctuations. They are almost identical to solutions from numerical MODFLOW models under identical settings. We then tested the ability of analytical solutions to inversely estimate aquifer properties such as hydraulic diffusivity by comparing to numerical simulation results for a broad range of parameter values. Reliable estimates of diffusivity can be achieved when choosing appropriate observation locations for the particular aquifer situation.

The analytical solutions proved to be fast, versatile and applicable for all types of boundary conditions provided they are continuous. Their implementation offers the opportunity to inversely estimate aquifer properties in a fast and efficient manner. For confined aquifer, diffusivity can be estimated at a level of less than 2% relative difference to numerical input data. This particularly holds for piezometer observations at intermediate distances from the open water body where the wave signal is not yet damped to strongly but has travelled through the aquifer sufficiently long to experience aquifer specifics. The longer the periodicity of the input wave signal, the further is this distance.

In case of hydraulic barriers, the confined aquifer solution can be used when the flow barrier shows conductivity differences to the aquifer of less than 2 orders of magnitude. For barriers with higher resistance, the analytical solution can be used when the input wave is a damped wave signal from a head observation behind the barriers but close to the open water body.

Leakage significantly impacts the propagation of the input wave signal into the aquifer for conductivity differences of the leaking unconfined layer of less than four orders of magnitude. In this case, the analytical solution including the confining layer resistance provides a tool to gain reliable estimates of diffusivity and resistance. However, due to the damping the observation location of the head signal for inverse estimation has to be carefully chosen being closer to the open water body the stronger the leakage, i.e. the lower the confined layer resistance.

Although we consider the simplified configuration of a 1D horizontal homogeneous confined/leaky aquifer, results can be applied to typical field situations. The scheme of deriving analytical solutions can easily be applied to more complex subsurface configurations providing the governing equations are linear. Examples are extending the solution for a 2-dimensional problem (Sun, 1997), including wave interference between aquifers (Li and Jiao, 2002) and a two-sided tidal wave problem (Sun et al., 2008).

Availability of data and code

Manuscript data and codes are freely available in the GitHub repository at https://github.com/AlrauneZ/WavePropagationAquifers (Zech and Hanckmann, 2022).

CRediT authorship contribution statement

Wout Hanckmann: Conceptualization, Methodology, Software, Writing - original draft. **Thomas Sweijen:** Conceptualization, Methodology, Data curation, Supervision. **Alraune Zech:** Conceptualization, Software, Supervision, Writing - review & editing.

Declaration of Competing Interest

The authors declare that they have no known competing financial interests or personal relationships that could have appeared to influence the work reported in this paper.

Acknowledgements

The authors further acknowledge and thank CRUX Engineering for their time investment in this research.

Appendix A. Supplementary data

Supplementary data associated with this article can be found, in the online version, at https://doi.org/10.1016/j.hydroa.2022.100125.

References

Bakker, M., Post, V., Langevin, C.D., Hughes, J.D., White, J.T., Starn, J.J., Fienen, M.N., 2016. Scripting modflow model development using python and flopy. Groundwater 54, 733–739. https://doi.org/10.1111/gwat.12413.

Bear, J., 1972. Dynamics of Fluids in Porous Media. Elsevier, New York.

EPA, U., 2008. EPA's Report on the Environment (Roe). U.S, Environmental Protection Agency, Washington, D.C.

Ferris, J.G., 1951. Cyclic fluctuations of water level as a basis for determining aquifer transmissibility. International Assoc. of Scientific Hydrology 33, 148–155.

Guo, H., Jiao, J.J., Li, H., 2010. Groundwater response to tidal fluctuation in a two-zone aquifer. J. Hydrol. 381, 364–371. https://doi.org/10.1016/j.jhydrol.2009.12.009.

Guo, Q., Li, H., Boufadel, M.C., Xia, Y., Li, G., 2007. Tide-induced groundwater head fluctuation in coastal multi-layered aquifer systems with a submarine outlet-capping. Adv. Water Resour. 30, 1746–1755. https://doi.org/10.1016/j.advwatres.2007.01.003.

Harbaugh, A.W., 2005. MODFLOW-2005, the U.S. Geological Survey modular groundwater model – the Ground-Water Flow Process. Technical Report 6-A16. U.S. Geological Survey Techniques and Methods.

Hemker, C., 1999. Transient well flow in layered aquifer systems: the uniform well-face drawdown solution. J. Hydrol. 225, 19–44. https://doi.org/10.1016/S0022-1694(99)00093-1.

Houben, G.J., 2015. Hydraulics of water wells-flow laws and influence of geometry. Hydrogeol. J. 23, 1633–1657. https://doi.org/10.1007/s10040-015-1312-8.

Ingersoll, L.R., Zobel, O.J., Ingersoll, A.C., 1948. Heat conduction: with engineering and geological applications. McGraw-Hill Book Company.

Jiao, J.J., Tang, Z., 1999. An analytical solution of groundwater response to tidal fluctuation in a leaky confined aquifer. Water Resour. Res. 35, 747–751. https://doi.org/10.1029/1998WR900075.

Kruseman, G., de Ridder, N. (Eds.), 2000. Analysis and Evaluation of Pumping Test Data, 47 ed. ILRI publication, Wageningen.

Li, H., Jiao, J.J., 2002. Analytical solutions of tidal groundwater flow in coastal two-aquifer system. Adv. Water Resour. 25, 417–426. https://doi.org/10.1016/S0309-1708(02)00004-0.

Nidzieko, N.J., 2010. Tidal asymmetry in estuaries with mixed semidiurnal/diurnal tides. J. Geophys. Res. Oceans 115, C08006. https://doi.org/10.1029/2009JC005864.

Nielsen, P., 1990. Tidal dynamics of the water table in beaches. Water Resour. Res. 26, 2127–2134. https://doi.org/10.1029/WR026i009p02127.

Sun, A.Y., Ritzi, R.W., Sims, D.W., 2008. Characterization and modeling of spatial variability in a complex alluvial aquifer: Implications on solute transport. Water Resour. Res. 44, W04402. https://doi.org/10.1029/2007WR006119.

Sun, H., 1997. A two-dimensional analytical solution of groundwater response to tidal loading in an estuary. Water Resour. Res. 33, 1429–1435. https://doi.org/10.1029/97WR00482.

Theis, C., 1935. The relation between the lowering of the piezometric surface and the rate and duration of discharge of a well using groundwater storage. Trans. Am. Geophys. Union 16, 519–524. https://doi.org/10.1029/TR016i002p00519.

Zech, A., Hanckmann, W., 2022. AlrauneZ/WavePropagationAquifers: v.1.0.2. Zenodo. https://doi.org/10.5281/zenodo.6308433.